

## Neon laser with wavelength $\lambda = 585.3$ nm pumped by pulsed inductive longitudinal discharge

© [A.M. Razhev](#),<sup>1</sup> [D.S. Churkin](#),<sup>1,2</sup> [R.A. Tkachenko](#)<sup>1,2</sup>

<sup>1</sup>Institute of Laser Physics of the Siberian Branch of Russian Academy of Sciences, Novosibirsk, Russia

<sup>2</sup>Novosibirsk State University, Novosibirsk, Russia

✉ e-mail: [churkin@laser.nsc.ru](mailto:churkin@laser.nsc.ru)

Received August 22, 2024

Revised February 11, 2025

Accepted February 12, 2025

The article presents the results of experimental studies of the energy, temporal, and spatial characteristics of the Penning neon laser generation ( $\lambda = 585.3$  nm) pumped by a pulsed inductive longitudinal discharge. A Ne–H<sub>2</sub> gas mixture was used as an active medium. The maximum generation energy of 0.14 mJ was obtained in a Ne:H<sub>2</sub> — 1:2 mixture. The radiation power reached 700 W with an optical generation pulse duration of 200 ns (FWHM). The laser beam had a cross-sectional shape close to a circle with a divergence of no more than 2 mrad. Based on the analysis of the amplitude-temporal characteristics of laser generation and inductive discharge current pulses, it is assumed that laser generation at a wavelength of 585.3 nm in a pulsed inductive longitudinal discharge occurs as a result of population of the upper laser level by electron impact, with Penning depopulation of the lower laser level by hydrogen molecules.

**Keywords:** pulsed inductive longitudinal discharge, Penning laser, yellow laser, inductive neon laser, pulsed power.

DOI: 10.61011/TP.2025.06.61374.258-24

### Introduction

Currently, laser radiation in the yellow region of the spectrum (550–590 nm) has many applications in biology and medicine, in particular, in ophthalmology [1]. Among its advantages are: an increased response during irradiation compared to the well-known lasers with the wavelengths of 532 and 633 nm [2–5], low scattering of the laser beam when passing through the refractive media of the eye, high exposure efficiency during coagulation of vascularized structures, lower pain, and etc. [6]. The effectiveness and safety of yellow lasers have been demonstrated in the treatment of a wide range of diseases, such as macular edema, post-thrombotic retinopathy, and central serous chorioretinopathy [7]. Commercial yellow lasers that exist today are mainly represented by optically pumped semiconductor lasers and dye-based lasers. The main drawbacks of these medical devices in the first case include low pulse power (no more than 2 W) and the inability to receive pulses shorter than 1  $\mu$ s. When using dye lasers, it becomes necessary to replace the dye frequently due to its burnout. Other medical devices used in this spectral region are based on copper vapor lasers. They have high values of both pulse and average power (about 10 W), however, they differ in rather large overall dimensions, high power consumption and low operating life (about 400–500 h) [8]. Thus, the issue of searching for alternative laser sources in the yellow region of the spectrum remains relevant. A pulsed inductive neon laser with radiation at a wavelength of 585.3 nm may be proposed as such a laser source.

A yellow-line neon laser with a wavelength of 585.3 nm corresponding to the transition of Ne I  $3p^2[1/2]_0 \rightarrow 3s^2[1/2]_1^o$  atoms is one of the most well-known Penning recombination lasers in which hydrogen or other additives serve as a quenching particle (e.g., NF<sub>3</sub>). The active medium of a plasma neon laser was intensively studied in the 80s and 90s. [9–12]XX. Both traditional longitudinal and transverse electric discharge and other methods, for example, an electron beam, were used to excite it [13,14]. In an electric discharge, the generation energy did not exceed 0.15 mJ [15] with optical pulse durations from units of nanoseconds to units of microseconds [15,16]. The pulse power of such laser systems, as a rule, was about tens of watts. The highest value was obtained in the study [16] and reached 1.1 kW. Probably, such energy characteristics caused a decline in interest in this active medium at that time. However, modern yellow lasers, used, for example, in micro-pulse trabeculoretraction, ensure exactly these laser generation parameters when acting on the internal tissues of the eye. Accordingly, as described above, a yellow neon laser may be considered as an alternative radiation source for medical applications.

Earlier in the work [17], we demonstrated the possibility of obtaining laser generation in the active neon medium with a wavelength of 585.3 nm when Ne–H<sub>2</sub> mixture is excited with a pulsed inductive cylindrical discharge. The system of generating a pulsed inductive discharge provided a high specific pumping power, however, it included an uncontrolled spark gap, which complicated the laser design and affected stability and service life. Consequently,

these drawbacks, combined with current trends aimed at miniaturizing laser sources, make it more preferable to use a longitudinal inductive discharge. Another pivotal issue is the recombination nature of neon laser generation with a wavelength of 585.3 nm, which makes it possible to use simpler systems for generating the pulsed inductive discharge based on a single switch in the form of a highly stable thyatron. The inductive discharge itself is formed as a result of electromagnetic induction in the absence of metal electrodes in an active medium. This advantage makes it possible to eliminate the typical drawbacks of conventional methods of pumping with longitudinal or transverse volume high-current electric discharge associated with spraying of material of the metal electrodes. Thus, the combination of absence of electrodes in the inductive discharge and the inertia of the active medium of the neon laser in the future will make it possible to create relatively simple laser sources from the engineering standpoint featuring high stability and a long service life. In this regard, the purpose of this work was to create a yellow spectrum neon laser with pumping by pulsed inductive longitudinal discharge.

## 1. Experimental setup

For the research, a system for generating a pulsed inductive discharge was used, made similar to a LC-inverter circuit (Fig. 1). This circuit consisted of a set of parallel-connected capacitors with capacitances  $C_1$  and  $C_2$ , which were charged from a Lambda EMI switching power supply ALE-152A to a preset voltage  $U_{ch}$ . After they have been charged the switch THY initiating the oscillating process in THY- $L$ - $C_1$  and THY- $L_a$ - $L$ - $C_2$  loops of the high-voltage circuit. Due to the difference in oscillation periods determined by the capacitive and inductive parameters of the electrical circuit, an operating mode was achieved in adjacent circuits where the voltage across the inductor had maximum values, exceeding the charge voltage by 1.5–1.7 times. A 300 mm long DT tube was used as an inductive laser emitter, having a working area with an internal diameter of the optical zone of about 8 mm and a bypass channel with a diameter of 20 mm, respectively.

An antenna-type inductor  $L$  was placed on the tube, made of four stranded wires PV6-Z with a cross section of  $10\text{ mm}^2$ . The laser resonator consisted of a dense mirror  $M_1$  with an aluminum coating ( $R > 90\%$ ) and a dielectric mirror  $M_2$  with  $R \sim 35\%$  at a wavelength of  $\lambda = 585\text{ nm}$ . Charge voltage  $U_{ch}$  in the experiments varied within 26–29 kV. The pulse repetition rate, depending on the pumping conditions, ranged from 1 to 100 Hz.

The spectral characteristics of spontaneous and laser radiation from a pulsed inductive longitudinal discharge in mixtures of neon with other gases were studied using spectrometer S-150 from Solar Laser Systems. The time characteristics of the generation pulses were studied using coaxial photocell FEK-15 with a time resolution of about 0.5 ns and photodiode FD-24K. The electrical pulses of

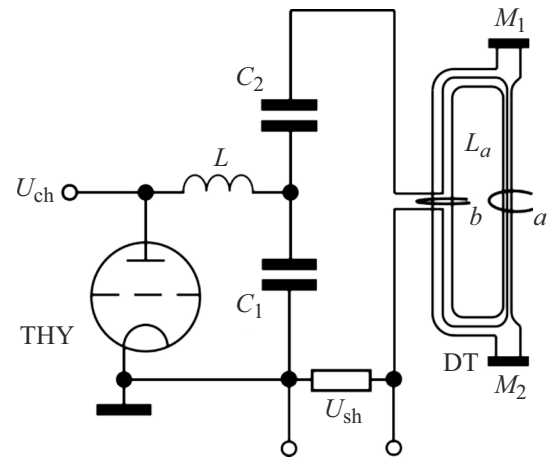


**Figure 1.** Electrical diagram of the Penning inductive neon laser pumping system.  $C_1 = C_2 = 97.2\text{ nF}$ , DT — discharge tube,  $L_a$  — inductor-antenna,  $L$  — inductance of buses and switch, THY — thyatron of TPI1-10k/50 series,  $U_{ch}$  = charging voltage 26–29 kV,  $M_1$  and  $M_2$  — resonator mirrors,  $a$  and  $b$  — location of Rogovsky belt during calibration and major measurements, respectively,  $U_{sh}$  — signal from the resistive current shunt.

the excitation system were recorded using high-voltage sensors Printek ACA-6039, a current resistive shunt and Rogovsky belt, the signals from which were sent to the digital storage oscilloscope Rigol MSO5354 with a 350 MHz band. Rogovsky belt was calibrated using the resistive shunt. To do this, the belt was placed on the tube so as to cover the plasma coil with the inductor (point  $a$  in Fig. 1), and at pressure of about 1 atm, when there was no inductive discharge, the signal was recorded from the resistive sensor and the Rogovsky belt simultaneously. Next, the belt was placed on the bypass channel in the area where the inductor was attached to the circuit (point  $b$  in Fig. 1), in order to remove the effect of the current through the inductor on the recorded signal and reduce the magnitude of the induced EMF. The energy characteristics of the generation were recorded using Ophir StarBright display with the measuring head Newport 919E -0.1-12- 25K. The spatial characteristics of the laser beam were studied using a digital camera Ophir Spiricon L11059.

## 2. Results and discussion

Experimental studies of the spectral characteristics of neon radiation when pumped by pulsed inductive longitudinal discharge have shown that laser generation at a wavelength of 585.3 nm occurs only in the presence of molecular hydrogen. The use of other additives in the form of gases such as  $\text{NF}_3$  and  $\text{SF}_6$  in two-component mixtures with neon under these pumping conditions led to a decrease in generation energy or its complete disappearance, as well as a redistribution of excitation energy between a whole set of the low-intensity lines in the visible region of the spectrum. In this regard, two-component gas mixtures

Ne–H<sub>2</sub> were used as the active medium at different ratios and partial pressures. Figure 2 shows the dependence of the generation energy and optimal pressure of a yellow neon laser on the percentage of neon in the active mixtures used at a pulse repetition rate of 1 Hz.

Maximal generation energy about 0.14 mJ was obtained at a ratio of Ne:H<sub>2</sub> — 1:2. The duration of the optical radiation pulses reached about 200 ns (FWHM), which corresponded to a pulse power of 700 W. The obtained generation characteristics turned out to be almost equal to the maximum results achieved when neon was excited by an electric discharge, and can subsequently be improved by further optimizing the excitation conditions. Fig. 2 also shows the dependence of optimal pressure of the mixture on the ratio of Ne:H<sub>2</sub>. Higher content of hydrogen in the mixture resulted in decrease of optimal pressure from 25 to 10 Torr at ratios Ne:H<sub>2</sub> — 1:1 and Ne:H<sub>2</sub> — 1:3 respectively. In the optimal composition Ne:H<sub>2</sub> — 1:2 laser generation was observed in the pressure range from 10 to 22 Torr with maximal radiation energy of 0.14 mJ at a pressure  $P_{\text{opt}}$  of about 17.5 Torr. Visual observations showed that the inductive discharge was steadily ignited up to the pressure of the active medium at 30 Torr.

Fig. 3 illustrates the oscillograms of optical pulses of neon laser radiation ( $\lambda = 585.3$  nm) at various pressures of the optimal gas mixture Ne:H<sub>2</sub> — 1:2. The shape of the optical pulses  $W$  depended on pressure and, as a rule, consisted of several peaks of varying intensity, the ratio of the amplitudes of which varied from pulse to pulse. At the same time, the most powerful pulses consisted of one pronounced peak, while the intensities of the other peaks were negligible.

At the same time, near the base, the generation pulses, regardless of the number of pronounced peaks, had almost the same duration of about 1  $\mu$ s. In all cases, the generation pulse occurred near the maximum of the inductive discharge current. Moreover, if the optical pulse consisted of several peaks, the moments of their appearance also coincided with the maxima of the current  $I$  or its derivative  $\frac{dI}{dt}$ .

In more detail, studies of the temporal behavior of spontaneous and laser radiation were carried out in the

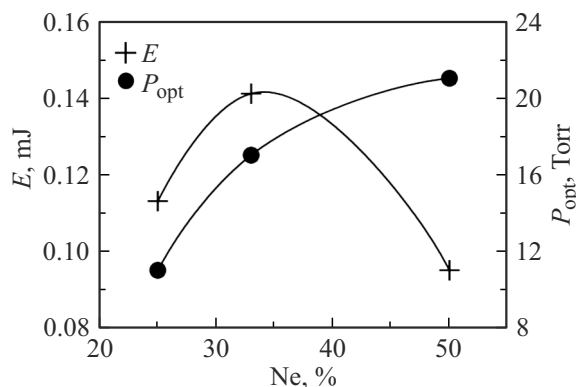


**Figure 2.** Generation energy and optimal pressure of a Penning inductive neon laser versus percentage of neon in Ne–H<sub>2</sub> mixture at a pulse repetition rate of 1 Hz.

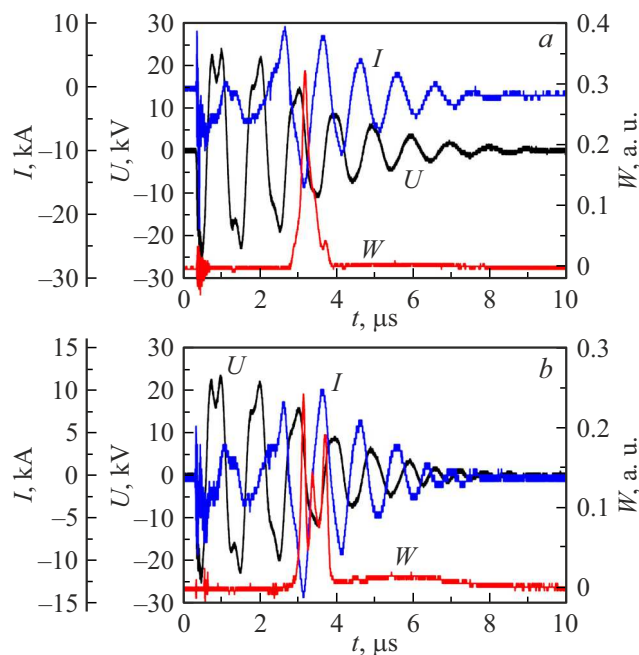


**Figure 3.** Voltage oscillograms on the inductor  $U$ , inductive discharge current  $I$  and optical pulses of spontaneous and laser radiation of Ne:H<sub>2</sub> mixture — 1:2 in the pulsed inductive discharge  $W$ :  $a$  — at optimal pressure 17.5 Torr;  $b$  — at low (14–15 Torr) pressure.

pressure range from fractions of Torr to the upper limit of the inductive discharge burning (Fig. 4). At low pressures, less than 1 Torr, the inductive discharge was ignited during the first half-cycle of voltage fluctuations across the inductor. There was a fairly high stability of inductive discharge ignition (at approximately the same time). No laser generation was observed in the mixture at such pressure level. A pulse of spontaneous radiation was recorded from the moment the inductive discharge was ignited, however, its greatest intensity was reached after the discharge had been quenched, then, the intensity declined drastically, ending in a low-intensity afterglow.

When the pressure increased to 8–10 Torr, a delay in the ignition of the inductive discharge became noticeable relative to the moment when the high-voltage switch THY was triggered and the oscillatory process in the inductor began: the inductive discharge began to ignite not on the first half-cycle, but on the second or third one. This may probably be due to the fact that the voltage across the inductor is no longer sufficient to cause a gas breakdown during the first half-cycle, yet a partial ionization of the gas mixture occurs, which subsequently acts as a preliminary ionization forming the initial conductivity. A weak peak of laser generation at a wavelength of 585 nm is noticeable at the leading edge of the spontaneous radiation pulse. Just as at lower pressures, the greatest intensity of spontaneous radiation was achieved by the time the inductive discharge had been quenched, however, at such pressures it is

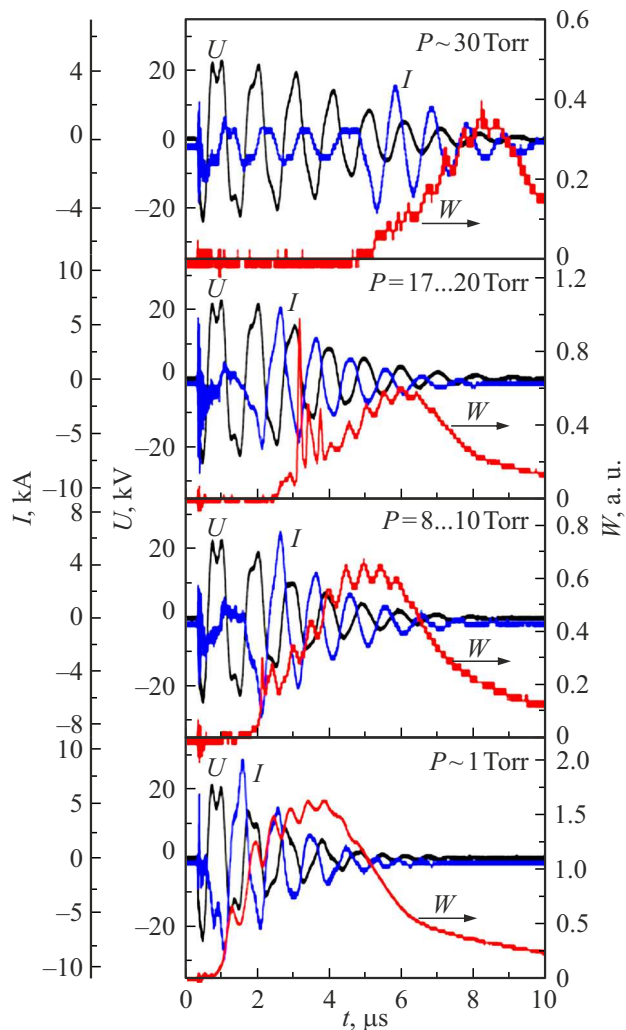


**Figure 4.** Pulses oscillograms: voltages on the inductor  $U$ , current of inductive discharge  $I$  and spontaneous and laser radiation  $W$  at various levels of pressure  $P$  of Ne:H<sub>2</sub> mixture — 1:2.

noticeable that during the direct ignition of the discharge, the intensity of spontaneous radiation was already noticeably lower.

Maximal generation energy at a wavelength of 585.3 nm was recorded at pressure of 17–18 Torr. In these conditions, the inductive discharge was ignited already in the third period of voltage fluctuations on the inductor, and the instability of the ignition led to the fact that the inductive discharge could ignite both at the beginning of the third period and at its the end. Just as at lower pressures, the generation pulse was observed at the leading edge of the optical pulse, while the main part of the spontaneous radiation pulse was observed already in the afterglow.

A further increase in pressure led to a break in generation. The inductive discharge was ignited after a significant delay and several voltage fluctuations on the inductor. Spontaneous radiation was recorded mainly during the discharge afterglow.

As noted above, the generation pulses were formed near the maximum of the inductive discharge current  $I$  or its derivative  $\frac{dI}{dt}$  in the case of complex shaped pulses consisting of several peaks. In addition, in these pumping conditions, a modulation of the amplitude of spontaneous radiation optical pulses was also observed, corresponding to a doubled frequency of oscillations of the inductor voltage (and the inductive discharge current), and a temporary shift of the peaks of the optical pulses oscillations relative to the peaks of the inductor voltage and the inductive discharge current. Such amplitude-time behavior of spontaneous radiation may be associated with changes in the temperature of electrons caused by their participation in kinetic processes with particles of the active medium. In paper [18], theoretical studies of the inductive discharge ignition modes at various operating (carrier) frequencies were carried out. The authors have highlighted three basic modes — quasi-steady-state, dynamic and high frequency modes differing by the ratio of the carrier frequency  $\omega = 2\pi f$  and specific frequency parameters of the inductive discharge, such as  $\nu_a$  and  $\nu_e$ . Parameter  $\nu_a$  corresponds to the characteristic time of the ions drift to the walls  $\tau_a = \nu_a^{-1}$ , and the parameter  $\nu_e$  corresponds to the characteristic time of the electron energy relaxation  $\tau_e = \nu_e^{-1}$ . Thus, the quasi-steady-state mode corresponds to the low-frequency case ( $\omega < \nu_a$ ), when the plasma density varies significantly during the period of current oscillations, and the electric field and electron temperature have a strongly nonlinear temporal behavior. At high frequencies when ( $\omega > \nu_e$ ), the electrons energy distribution function (EEDF) and electrons temperature is stable for a certain period and is determined by the electrical field  $E = E_0(1 + \omega^2/\nu_{\text{eff}}^2)^{1/2}$ , where  $E_0$  — electrical field in DC plasma with similar geometry of the discharge gap and gas pressure, and  $\nu_{\text{eff}}$  — electrons collision effective frequency. The intermediate case ( $\nu_a < \omega < \nu_e$ ) corresponds to the so-called „dynamic mode“, where plasma density varies slightly during the oscillation period, while the electron temperature, ionization rate, and type of EEDF can vary significantly during the period. An analysis of calculation results carried out in this paper suggests that in the frequency range 0.5–1 MHz, corresponding to our pumping conditions, a dynamic mode is realized, and during the period of electric field oscillations, the electron temperature can vary within 20%–30%, while, in general, the concentration of electrons remains almost constant.

A similar pattern was outlined in [19], where maximum electron temperatures in plasma of the inductive discharge with ferromagnetic amplification was reached at the same time when maximum values of the electric field strength were reached, whereas minimum values were reached when the electric field strength passed through zero. At the same time, just as in [18], there was a delay in the position of the electron temperature minima relative to zero value of the electric field strength. This is due to the fact that the electrons temperature fluctuations in plasma are caused by the energy losses during elastic and inelastic collisions with atoms of the plasma-forming gas, and relatively small field

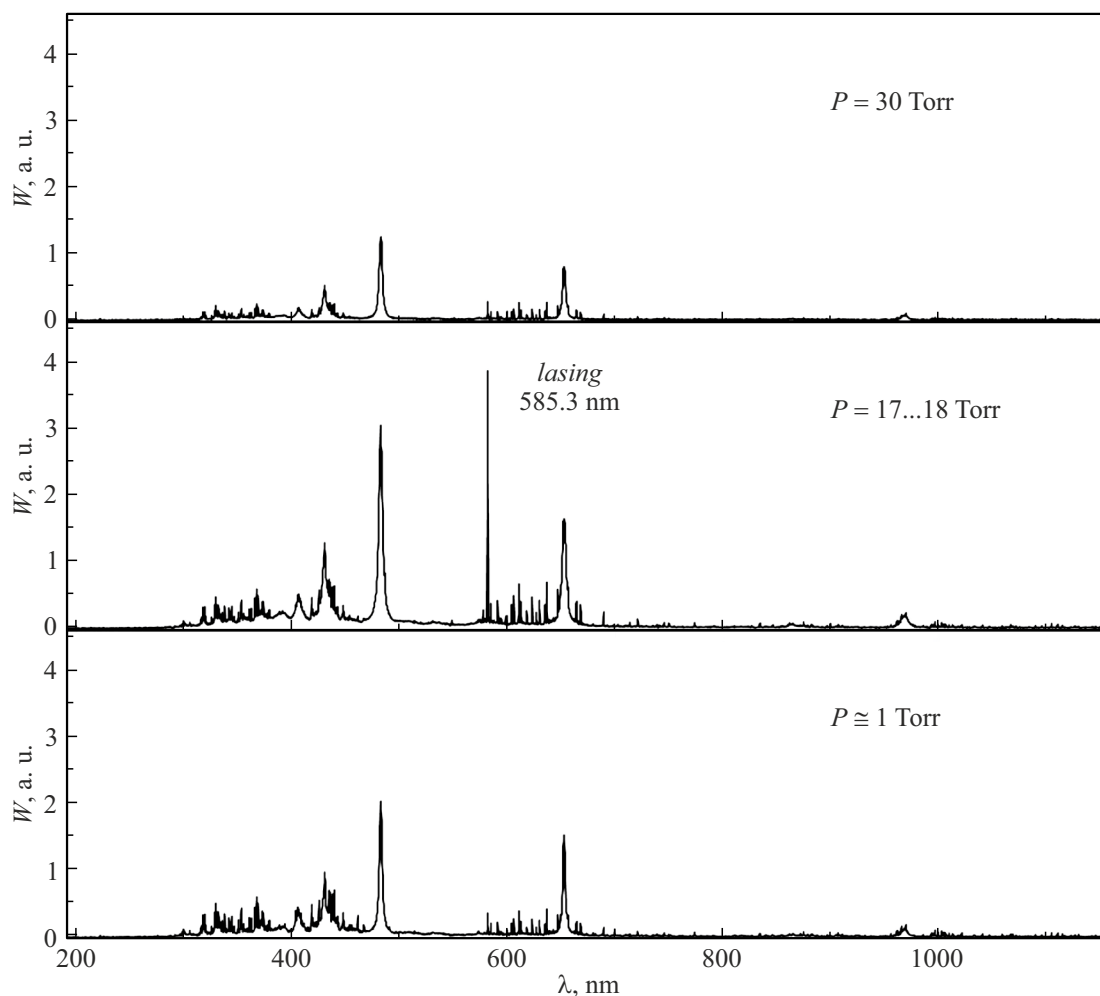


**Figure 5.** Spectra of Ne–H<sub>2</sub> mixture radiation — 1:2 in the pulsed inductive longitudinal discharge at various levels of pressure  $P$  from 1 to 30 Torr.

values are insufficient to compensate for the electron energy losses; the electron temperature, accordingly, continues to decline when the electric field strength passes through zero. Thus, it can be stated that the observed temporal behavior of spontaneous radiation generally reflects the processes characteristic of inductively coupled plasma.

The spectrum of spontaneous radiation of Ne:H<sub>2</sub> mixture — 1:2 consisted of a large number of lines, mainly in red and blue-ultraviolet regions of the spectrum (Fig. 5). In the red region of the spectrum, the strongest lines were attributed to  $3p \rightarrow 3s$  neon transitions. In the blue and ultraviolet regions, the presence of lines related to  $4p \rightarrow 3s$  transition of neon are seen, as well as several lines related to  $4d \rightarrow 3p$  and  $3p \rightarrow 3s$  transitions of Ne<sup>+</sup> ions. There were also quite intense Balmer lines H <sub>$\alpha$</sub> , H <sub>$\beta$</sub>  and H <sub>$\gamma$</sub>  in the spectrum. With an increase in pressure from 1 Torr, the spectral composition of spontaneous radiation practically did not change, in fact, a gradual decrease in the intensity of all lines was observed. At the same time, a decrease in pressure below 1 Torr led to occurrence of a fairly powerful generation at a wavelength of 1114.3 nm, corresponding

to the transition  $4s^2[3/2]_1^o \rightarrow 3p^2[5/2]_2^o$  of neon. The generation energy on this line exceeded 0.01 mJ, but its duration could not be measured due to the insufficient sensitivity of the devices in this spectral region. At a pressure of less than 0.1 Torr on the red lines the neon was generated with wavelengths of 630.4 nm and 650.6 nm, respectively. Separate experiments are scheduled for a more detailed study of generation in this area. It is worth noting that laser generation in the red region on the above-mentioned lines occurred only in the presence of additives, while the addition of helium to pure neon or Ne–H<sub>2</sub> mixture had the greatest effect. In a single-component neon environment, laser generation did not occur on these lines in this pumping system.

In addition to direct recording of laser and spontaneous radiation of neon, the spontaneous radiation spectrum was recorded from the side of a transparent capillary tube. In these experiments (correction for probable absorption of UV radiation by the tube material) in the active medium of pure neon at optimal pressures 17–20 Torr the radiation spectrum consisted mainly of red lines related to  $3p \rightarrow 3s$

transitions of Ne. When hydrogen was added it resulted in almost complete disappearance of these lines; when the radiation was detected from the side, only the lines belonging to the Balmer series were distinguishable in the spectrum. The results obtained correlate with the conclusions in paper [9], where the authors conclude that hydrogen additives reduce the population not only of the lower, but also of the upper laser level, while the appearance of laser generation at a wavelength of 585.3 nm is possible only with certain ratios of Ne–H<sub>2</sub> mixture.

For classical longitudinal electric discharge and hollow cathode discharge, detailed studies of the mechanisms of population inversion formation at transition  $3p^2[1/2]_0 \rightarrow 3s^2[1/2]_1^o$  of neon were carried out, which are described in paper [20]. Various modes of operation were considered in this paper, mainly differing in the amplitude and duration of the discharge current. At small (less than 1  $\mu$ s) durations of the discharge current, laser generation at a wavelength of 585.3 nm was observed mainly in the afterglow, while at long durations and amplitudes of the pumping current, laser generation could occur during ignition of the discharge. In this case, the upper laser level can be pumped by an electron impact. At the same time, the appearance of laser generation in the afterglow during neon excitation in the longitudinal electric discharge and hollow cathode discharge occurs mainly due to pumping of the upper laser level because of the triple recombination of neon ions. The authors also established the selective nature of the depopulation of the lower laser level due to the Penning reaction in collisions of neon with hydrogen molecules. In our case, theoretical studies and additional experiments are scheduled for detailed studies of plasma chemical reactions in the pulsed inductively coupled plasma. Based on the experimental results already obtained, we can assume that laser generation at a wavelength of 585.3 nm in a pulsed inductive longitudinal discharge occurs as a result of populating the upper laser level with an electron impact, followed by Penning depopulation of the lower laser level with hydrogen molecules.

In cross-section, the laser beam had a shape close to circular (see yellow, Fig. 6) with a maximum intensity in the central part, which makes it possible to control the spatial characteristics of the beam by using various types of resonators. The divergence was found as  $\theta = \arctg((d_L - d_0)/L)$  (where  $L$  — distance from the output mirror,  $d_L$  — diameter of section at half maximum for this distance  $L$ ,  $d_0$  — diameter of section at half maximum near the front mirror  $M_1$  (Fig. 1)). The results of the measurements carried out in this way showed that the divergence is  $(2 \pm 0.2)$  mrad.

Separate studies of laser operation in the repetitively-pulsed mode were conducted. For the described pumping system, with an increase in the pulse repetition rate to 10 Hz, maximum generation energy practically did not change and remained at the level of 0.14 mJ/imp. A further increase in frequency led to a decrease in the generation energy, as well as an increase in the instability of the inductive neon

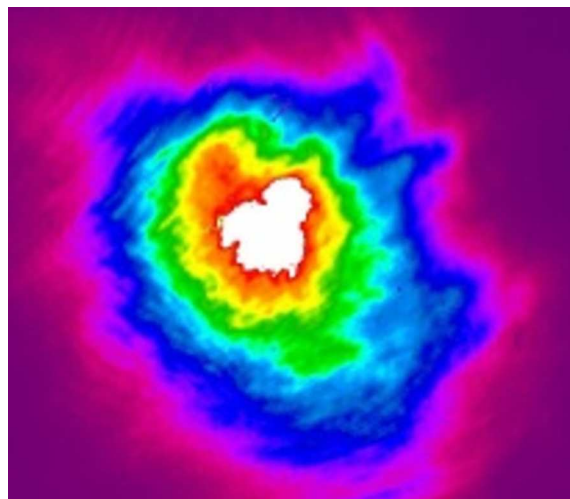


**Figure 6.** Profile of Penning inductive neon laser beam ( $\lambda = 585.3$  nm) in cross-section.

laser, which may be due to overheating of the laser tube. The negative effects of this factor were taken into account when developing a similar high-voltage circuit (Fig. 1) with the same inductive emitter and high-voltage switch, but with reduced capacitances, which helped to diminish the amount of stored energy. In these conditions, the generation energy decreased to 1.5–2  $\mu$ J, but its value remained almost unchanged up to the pulse repetition rate of 100 Hz. Thus, the subsequent optimization of the pumping conditions of this laser system will lead to a possibility of creating small-sized yellow lasers for practical applications.

## Conclusion

As a result of research, the possibility of pumping the active medium of a Penning neon laser with a pulsed inductive longitudinal discharge was demonstrated. Laser generation in the yellow region of the spectrum ( $\lambda = 585.3$  nm) was obtained in mixtures of neon and molecular hydrogen at different ratios. It is assumed that the main mechanism for the laser generation to occur at a wavelength of 585.3 nm in a pulsed inductive longitudinal discharge is populating the upper laser level with an electron impact followed by Penning depopulation of the lower laser level by hydrogen molecules. The generation energy reached a value of 0.14 mJ with a radiation power of 700 W with a duration of optical pulses of 200 ns (FWHM), which corresponds to the maximum results achieved in an electric discharge. The laser beam in cross-section had a shape close to a circle, with a divergence of no more than 2 mrad. A repetitively-pulsed mode of laser operation with an average power of up to 0.2 mW has been implemented.

## Funding

The work was supported by the Ministry of Science and Higher Education of the Russian Federation (project No. 121033100059-5).

## References

- [1] A.F. Yusupov, Sh.A. Djamalova, Z.A. Makhmudova. Adv. Ophthalmology, **3** (3), 189 (2023). DOI: 10.57231/j.ao.2023.3.3.044
- [2] E. Özmert, S. Demirel, Ö. Yanık, F. Batıoğlu. J. Ophthalmology, **2016** (1), 1 (2016). DOI: 10.1155/2016/3513794
- [3] V. Kapoor, V. Karpov, C. Linton, F.V. Subach, V.V. Verkhusha, W.G. Telford. Cytometry Part A, **73A** (6), 570 (2008). DOI: 10.1002/cyto.a.20563
- [4] V. Kapoor, F.V. Subach, V.G. Kozlov, A. Grudin, V.V. Verkhusha, W.G. Telford. Nat. Methods, **4** (9), 678 (2007). DOI: 10.1038/nmeth0907-678
- [5] W.G. Telford, T. Hawley, F. Subach, V. Verkhusha, R.G. Hawley. Methods, **57** (3), 318 (2012). DOI: 10.1016/j.ymeth.2012.01.003
- [6] M.K. Adam, B.M. Weinstock, K.K. Sundeep, D.S. Ehmann, J. Hsu, S.J. Garg, A.C. Ho, A. Chiang. Ophthalmol Retina, **2** (2), 91 (2018). DOI: 10.1016/j.oret.2017.05.012
- [7] K.E. Gosteva, N.N. Gosteva. Laser Medicine, **25** (3S), 70 (2021). DOI: 10.37895/2071-8004-2021-25-3S-70
- [8] A.A. Asratyan, M.A. Kazaryan, N.A. Lyabin, I.V. Ponomarev, V.I. Sachkov, H. Li. *Laserniye sistemi na osnove parov metalllov dlya primeneniya v meditsine* (RAS, M., 2017) (in Russian), DOI: 10.15518/isjaec.2018.31-36.097-120
- [9] D. Schmieder, D.J. Brink, T.I. Salamon, E.G. Jones. Opt. Commun., **36** (3), 233 (1981). DOI: 10.1016/0030-4018(81)90362-X
- [10] M.I. Lovaev, V.F. Tarasenko. Sov. J. Quant. Electron., **18** (10), 1237 (1988). <https://www.mathnet.ru/eng/qe12468>
- [11] M.I. Lomaev, D.Yu. Nagornyi, V.F. Tarasenko, A.V. Fedenev, G.V. Kirillin. Sov. J. Quant. Electron., **19** (10), 1321 (1989). DOI: 10.1070/QE1989v019n10ABEH009234
- [12] A.N. Panchenko, V.F. Tarasenko. Sov. J. Quant. Electron., **20** (1), 24 (1990). DOI: 10.1070/QE1990v020n01ABEH004783
- [13] F.V. Bunkin, V.I. Derzhiev, G.A. Mesyats, V.S. Skakun, V.F. Tarasenko, S.I. Yakovlenko. Sov. J. Quantum Electron., **15** (2), 159 (1985). DOI: 10.1070/QE1985v015n02ABEH006095
- [14] P.A. Bokhan, D.E. Zakrevskii, V.I. Mali, A.M. Shevnin, A.M. Yancharina. Sov. J. Quant. Electron., **19** (6), 719 (1989). DOI: 10.1070/QE1989v019n06ABEH008116
- [15] I.I. Murav'ev, E.V. Chernikova, A.M. Yancharina. Sov. J. Quant. Electron., **19** (2), 123 (1989). DOI: 10.1070/QE1989v019n02ABEH007733
- [16] I.M. Boichenko, A.N. Panchenko, A.E. Telminov, A.A. Fedenev. Bull. Lebedev Phys. Inst., **35** (5), 142 (2008). DOI: 10.3103/S1068335608050047
- [17] A.M. Razhev, D.S. Churkin, R.A. Tkachenko. Laser Phys. Lett., **18** (9), 1 (2021). DOI: 10.1088/1612-202X/ac1609
- [18] V.I. Kolobov, V.A. Godyak. Plasma Sources Sci. Technol., **26**, art. 075013 (2017). DOI: 10.1088/1361-6595/aa7584

- [19] M.V. Isupov, V.A. Pinaev. Prikladnaya mekhanika i tekhnicheskaya fizika, **64** (5), 27 (2023) (in Russian). DOI: 15372/PMTF202315321
- [20] E.L. Latush, M.F. Sem, G.D. Chebotarev. Sov. J. Quant. Electron., **20** (11), 1327 (1990). DOI: 10.1070/QE1990v020n11ABEH007496

Translated by T.Zorina